Proceedings of the 3rd Marine Energy Technology Symposium
METS2015
April 27-29, 2015, Washington, DC

EXPERIMENTAL AND NUMERICAL ANALYSIS OF A SMALL ARRAY OF 45:1 SCALE HORIZONTAL AXIS HYDROKINETIC TURBINES BASED ON THE DOE REFERENCE MODEL 1

Teymour Javaherchi
University of Washington - NNMREC
Seattle, WA, USA

Nick Stelzenmuller
University of Washington - NNMREC
Seattle, WA, USA

Alberto Aliseda*
University of Washington - NNMREC
Seattle, WA, USA

ABSTRACT

We present results from an experimental/numerical comparison of energy extraction efficiency and wake flow field characteristics in a small array of three scale-model (45:1) Horizontal Axis Hydrokinetic Turbines (HAHT). The model turbine was designed based on the DOE Reference Model 1 (DOE RM1), with a modified geometry to reproduce performance at the flume scale Reynolds numbers (10^5). These modifications were necessary to overcome the strong Reynolds number dependency of the NACA6*xxxx* airfoil family, used on the original RM1 design for its cavitation properties, and therefore on the device performance in experimental analysis. The performances and wakes of three turbines placed in a variety of array configurations were analyzed through a combination of experimental measurements and Computational Fluid Dynamics (CFD) modeling. Where possible, the results from experiments and simulations are compared to validate the simulations and understand the limits of the physics captured in the simulations. Once validated, details of the rotor flow field that could not be fully resolved by the experimental measurements are visualized from the numerical solution of the RANS equations to interpret the complex turbine-wake interactions in the experimental results.

INTRODUCTION

Marine HydroKinetic (MHK) turbines require engineering methods that can provide quantitative answers to open questions regarding their performance, optimization, and environmental effects. These advanced design, evaluation and optimization methods can speed up the development process from concept to prototype to pilot demonstrator, and reduce the capital requirements of this incipient industry.

Previous studies [1, 2, 3, 4, 5] have addressed some of these questions by either numerical simulation or laboratory experiments using a wide range of turbine geometries. The creation of the DOE Reference Model 1 (DOE RM 1) reference turbine geometry allows for direct comparison of results and analysis from different research groups in an open dialog that can benefit this community. Here, the numerical simulations and experimental results using a modified version of this reference model, operating in the same range of Tip Speed Ratios (TSR) as the original DOE RM1, to study the performance and wake hydrodynamics of this Horizontal Axis Hydrokinetic Turbine (HAHT) is presented.

Laboratory-scale testing of HAHT is used to validate numerical models and gain insight into the performance and wake dynamics of HAHT. Recirculating flumes and towing tanks are used for these tests, with measurements of the torque produced at the shaft, the rotational speed, and the drag (or thrust) force on the HAHT, as well as the flow velocity field. Multiple experimental studies in the literature [6,7,8] have measured a variety of turbine performance metrics and wake structure, to characterize the performance of single HAHT with various rotor geometries. These studies typically provide insight into the fluid dynamics and energy conversion process of MHK turbines, although unfortunately through incomplete information that limits the certainty and quantitativeness of the conclusions.

The DOE Reference Model 1 (DOE RM 1) was proposed as an open source design for HAHT that could be used to benchmark computational and experimental studies. Lawson et al. [3] have performed a detailed numerical analysis on the DOE RM1 model using RANS simulation with a rotating frame turbine implementation, as well as with a sliding mesh implementation that

*Corresponding Author: aaliseda@u.washington.edu

included the two side-by-side turbines and the central support column. They investigated the effect of mesh resolution on numerical modeling results and characterized the turbine performance using both steady and transient models, showing good agreement between unsteady and steady simulations for the optimal operating conditions (TSR =6.3 and $\theta_p = 0°$), where the flow is fully attached to the turbine blade. They did find, however, that for other operating conditions, unsteady models might be the better choice in order to provide more accurate results for the flow field and turbine performance characterization in situations where the flow is separated in a significant part of the blade suction surface.

EXPERIMENTAL SETUP AND ANALYSIS METHODS

Preliminary experiments were conducted with a laboratory turbine (maximum power 30W) that used the DOE Reference Model 1 (DOE RM 1) rotor [9] at a 45:1 scale. Measurements conducted in a large scale flume (1 m^2 cross section, 1.2 m/s free stream velocity) showed a low coefficient of performance ($C_p^{maximum} \approx 20\%$) for this 45:1 geometrically-scaled DOE RM1 rotor, compared to predictions for the the full-scale DOE RM1 performance based on Blade-Element-Momentum Theory ($C_p^{maximum} \approx 45\%$).

The relatively poor performance of the geometrically-scaled rotor was determined to be a Reynolds number effect; specifically associated to the sharp decrease in foil performance at some critical Reynolds number due to laminar separation bubble dynamics, as described by Lissaman [10]. To remove this Reynolds number dependency, the geometrically scaled model was redesigned using a different family of NACA airfoils (4415). The modifications were done such that the scaled model would still operate under the same range of TSR and match the performance of the full scale DOE RM 1.

Rotor and nacelle design

The redesigned rotor maximizes the local Reynolds number along the blade, within the constraints of matching the optimum TSR of the full-scale rotor and the maximum rotor diameter that could be tested in the flume at a reasonable blockage ratio. Figure 1 shows the local Reynolds number along the blade span at several free-stream flow speeds for the geometrically-scaled DOE RM1 with solid lines and the modified rotor with dashed lines. The foil section used in the DOE RM1 is the NACA 63424 foil, for which the critical Reynolds number is estimated to be at 10^5; the foil used in the redesigned rotor was the NACA 4415 foil, chosen as a compromise between structural integrity and experimentally demonstrated performance at low Reynolds numbers (the critical Reynolds number for this airfoil has been measured at 7 10^4). The open source design code HARP−Opt [11] was used with NACA 4415 experimental wind tunnel data to optimize chord and twist distributions. Details of the modified laboratory-scale rotor design, nacelle design, instrumentation, and testing procedure are given in [9].

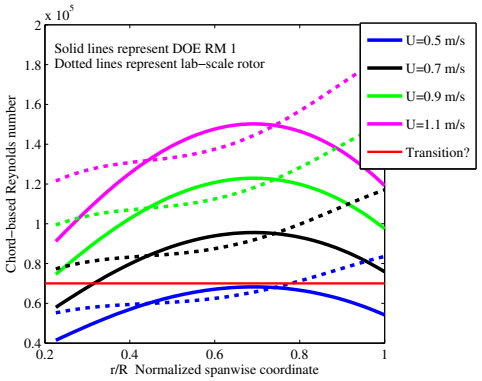

FIGURE 1. LOCAL REYNOLDS NUMBER ($\frac{U_R C}{\nu}$, WHERE C IS THE CHORD LENGTH, U_R IS THE RELATIVE VELOCITY, AND ν IS THE KINEMATIC VISCOSITY) ALONG THE SPAN OF THE BLADE, PLOTTED FOR THE GEOMETRICALLY-SCALED DOE RM1 (TRANSITION AT $\approx$ $RE = 10^5$) AND THE MODIFIED LABORATORY-SCALE ROTOR (TRANSITION AT $\approx RE = 7\ 10^4$) FOR VARIOUS FREESTREAM VELOCITIES AT TSR=7.

The modified 45:1 scale model consists of a 0.45 m diameter turbine rotor manufactured on a CNC mill from aluminum and a 0.1 x 1 m cylindrical nacelle. The nacelle contains a torque sensor (TFF325 Futek, Irvine, CA), magnetic encoder (RM22 RLS, Komenda, Slovenia), and a magnetic particle brake (Placid Industries, Lake Placid, NY) used to apply shaft loading. The torque sensor and magnetic encoder are wired to an analog-digital converter and acquisition system (PCIe-6341 National Instruments, Austin, Texas) sampled at 1000 Hz. The turbine model is mounted to a vertical post extending from the bottom of the flume to the nacelle. The turbine CAD model is shown in Figure 2.

Laboratory Setup

Flume testing was carried out at the Bamfield Marine Science Center, with a 1 m wide by 0.8 m depth cross sectional profile and 12.3 m long test section. The blockage ratio was 20%. ADV (Vector Nortek, Oslo, Norway) and PIV (LaVision Gmbh., Goettingen, Germany) systems were used to characterize the flow in the array, within the predefined interrogation windows aligned parallel to the flow and on the axis of rotation of the turbine, as shown in figure 3. PIV data was taken for 40 seconds at 5 Hz for each imaging location and the results processed un-

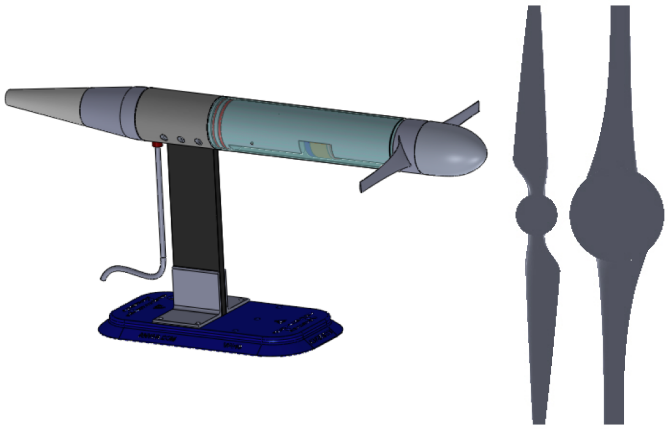

FIGURE 2. CAD MODEL OF THE MODIFIED SCALED HAHT FORM THE DOE RM 1 GEOMETRY AND COMPARISON OF THE ORIGINAL DOE RM1 ROTOR WITH THE REDESIGNED ROTOR WITH HIGHER CHORD-BASED REYNOLDS NUMBER..

der the assumption of statistically steady free-stream flow. The velocity fields 2 diameters upstream of each turbine and 2, 3, 5 and 7 diameters downstream of each turbine were measured from PIV at vertical-streamwise planes that covered the flow from the centerline to very near the free surface. These measurements were averaged over the interval of acquisition (60 s) and along the streamwise coordinate inside each PIV domain, that is for all the measurement points that are at the same distance from the turbine axis of rotation.

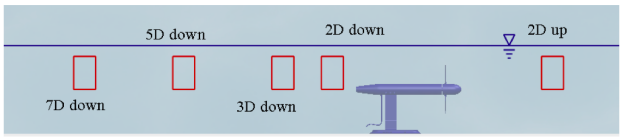

FIGURE 3. PIV IMAGING WINDOWS FOR MEASUREMENT OF VELOCITY UP- AND DOWNSTREAM OF THE TURBINE DURING THE EXPERIMENT.

Numerical Analysis

The Blade Element Model (BEM) was used for performance and wake characterization of the laboratory-scale model turbine array. This methodology was previously validated to characterize the performance and flow field associated with a horizontal axis wind turbine (NREL Phase VI) [12, 13]. The BEM formulation is combined with the RANS equations and a $\kappa-\omega$ *SST* turbulence closure model to investigate the effect of the Tip Speed Ratio variation (TSR=5.5 to 10.3) and array configuration on the performance and wake structure of the three rows of turbines.

RESULTS

Figure 4 presents the comparison between the experimental measurements and numerical predictions of the performance in a two turbine array. The results agree well for the turbines at or near the optimum TSR (≈ 7.2) but deviate slightly for lower TSR values, demonstrating that CFD becomes less accurate when the operating conditions of the turbines are such that separated flow is present in a significant span of the blade.

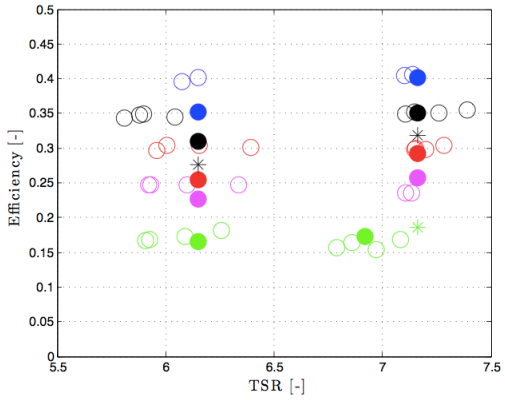

FIGURE 4. COMPARISON OF NUMERICAL PREDICTIONS (FULL SYMBOLS) VS EXPERIMENTAL MEASUREMENTS (EMPTY SYMBOLS) OF THE PERFORMANCE OF TWO TURBINES PLACED COAXIALLY WITH 5 (GREEN), 8 (MAGENTA), 11 (RED) AND 14 (BLACK) DIAMETERS DOWNSTREAM SEPARATION. BLUE SYMBOLS ARE USED FOR THE FRONT TURBINE UPSTREAM.

The discrepancy in the efficiency between experiments and computations at lower TSR, from 5-7, brings about interesting information on the dynamics of the turbine rotor. It is interesting to note that the experimentally measured efficiency is almost constant for a wide range of TSR values, decreasing from the theoretical peak around 7 to about 5.5 with little change in performance. This is in contradiction with aero- and hydrodynamic principles: decrease in TSR will result in the increase of AOA along the blade span. Large AOA values result in flow separation and unsteadiness along the blade span, and eventually stall, especially close to the root of the blade. These phenomena should decrease the efficiency of the turbine. Further analysis of the experimental data showed that, when the turbine operates under

lower TSRs conditions, there is an increase in fluctuations of the rotational velocity, which affects the flow structure at the blade surface, and therefore rotor performance [9].

Figure 5 shows the temporal variation of the turbine's rotational velocity at the two ends of the TSR range explored (TSR=5 and 10). The blue and green curves show the temporal variation of rotational speed normalized with the mean for TSRs equal to 5 and 10, respectively. It confirms that at TSR=10, the rotational speed has small fluctuations, while at lower TSR the fluctuations are relatively large and there are even a few large excursions (beyond 3 times the signal rms) during the 60 seconds of measurements. Our hypothesis is that these large fluctuations in the rotational velocity translate into rapid fluctuations in the value of AOA along the blade span. These rapid changes in AOA values would increase the stall angle along the blade span and therefore would postpone the potential stall at low TSR values (high AOA values). The result of this dynamic effect is that the efficiency of the turbine remains high as the TSR value decreases and the turbine still performs close to its maximum efficiency.

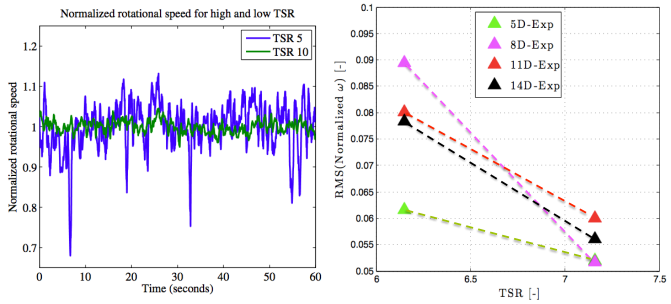

FIGURE 5. TEMPORAL VARIATION OF MEASURED NORMALIZED ROTATIONAL SPEED OF TURBINE DURING TWO EXTREME END OF TSR RANGE (TSR=5 AND 10).

Figure 6 presents the results from a coaxial array, at 5 diameters downstream separation. Consistently with the results from the two turbine array, the computational results agree well with the experimental measurements for the optimum TSR value, but the agreement decays for lower TSR. The experiments show a remarkably constant power coefficient for a range of TSR from 5-7, while the numerical simulations predict the theoretical drop in performance as the TSR moves away from the optimum and the angle of attack along the span increases above the value of maximum lift and into stall.

The most remarkable observation from the efficiency results, in a three turbine coaxial array, is that the downstream-most turbine produces more power and has a higher efficiency than the middle turbine. This is apparently contradictory with the idea that as the flow goes through each of the turbine rotor disks, it loses momentum to the energy extraction by the blades, and therefore the kinetic energy flux reaching the turbines directly behind will decrease. The confinement in the flume, however, at a geometrical blockage ratio of 20%, forces the low momentum flow to mix with the high momentum flow around the turbine disk, reducing the momentum deficit quickly. This was observed in the PIV velocity profiles behind the turbines (not shown) where the momentum deficit recovery in the experiments was much higher than expected. The mixing produced by the presence of the middle turbine leads to an increased momentum flux (not decreased as would seem intuitive in an infinite domain) into the disk of the downstream-most turbine, and the result is a higher power and efficiency in the downstream-most turbine compared to the middle turbine located 5D upstream of it.

To confirm this rationale for the non-monotonic trend of efficiency with downstream location of the turbines in the array, we show the Turbulent Kinetic Energy contours computed from the BEM simulations in the three turbine coaxial array (Figure 7). This result clearly demonstrate that the contribution of the middle turbine to the Turbulent Kinetic Energy in the wake is significant and, in this highly confined flow, results in enhanced mixing of high momentum flow with the wake. The net result is a higher kinetic energy flux, obtained by integrating the cube of the flow velocity along the cross section of the rotor disk, in the downstream-most turbine (0.437 V_∞^3) compared to the middle turbine (0.387 V_∞^3).

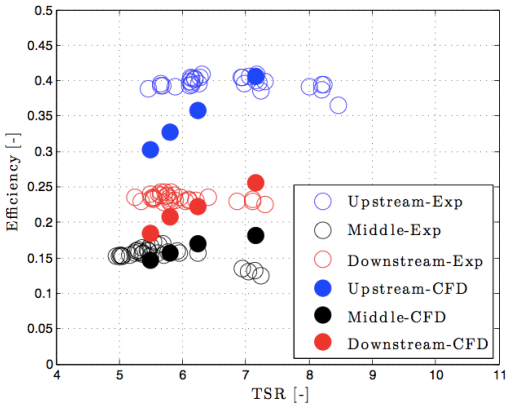

FIGURE 6. COMPARISON OF NUMERICAL PREDICTIONS (FULL SYMBOLS) VS EXPERIMENTAL MEASUREMENTS (EMPTY SYMBOLS) OF THE PERFORMANCE OF THREE TURBINES PLACED COAXIALLY WITH 5 DIAMETERS DOWNSTREAM SEPARATION. FRONT TURBINE: BLUE SYMBOLS, MIDDLE TURBINE: BLACK SYMBOLS, DOWNSTREAM TURBINE: RED SYMBOLS.

The results from the three turbine array with lateral offset

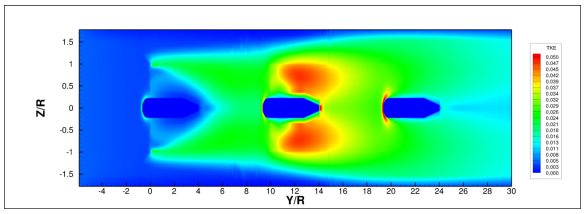

FIGURE 7. CONTOURS OF TURBULENT KINETIC ENERGY IN THE MID PLANE OF THE FLOW IN A THREE TURBINE COAXIAL ARRAY. NOTE THAT THE HIGH TURBULENT INTENSITY IN THE WAKE OF THE MIDDLE TURBINE WILL LEAD TO INCREASED MIXING OF HIGH MOMENTUM FLOW INTO THE WAKE AND A HIGHER KINETIC ENERGY FLUX IN THE DOWNSTREAM-MOST TURBINE COMPARED TO THE MIDDLE TURBINE (0.437 VS 0.387 RELATIVE TO THE FREE STREAM VALUE)

between the turbines show the same tendencies of agreement at optimum TSR, with an almost constant performance in the experiments and a marked decrease with TSR in the simulations. There is an interesting trend that appears from these results and that is not observed in the previous data, probably because of the range of TSR explored here. The simulations do not predict an optimum value of Cp for a TSR between of 7 and 7.5, as is the case in the experiments, and is predicted by the BEM theory. Rather the performance keeps increasing and peaks at a TSR that is different for each turbine in the array (TSR=8 for the front turbine, TSR=8-8.5 for the middle turbine, and no maximum detected for the downstream-most turbine).

It is important to note that the efficiency in the numerical simulations rises above the experimental values, particularly as the TSR exceeds the theoretical optimum and the efficiency keeps increasing rather than peaking at that value. This indicates that the blockage ratio from the flume, approximately 20%, has a cumulative effect in the array testing, particularly for the turbines with lateral offset, where the turbines operate very near the flume walls. The blockage ratio increases the performance artificially, due to the forced flow through the turbine rotor disk, rather than bypassing it, and it increases the value of the TSR for optimum performance, as it accelerates the flow through the turbine disk, with respect to the velocity of the flow with an infinitely wide cross section, effectively increasing the value of V and therefore the value of ΩR necessary to achieve an optimum distribution of angle of attack.

To test this hypothesis, we perform simulations with an increased cross section of the computational domain. We double and quadruple the cross section of the domain, to reduce the blockage ratio to 10% and 5%. Figure 9 presents the results of the study with three turbines at a lateral offset of 0.25D and a downstream separation of 5D, at 3 different levels of blockage ratio.

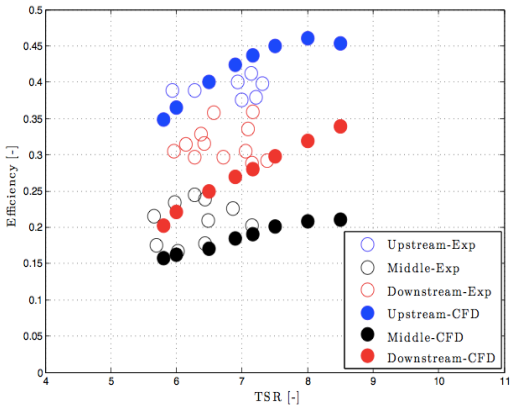

FIGURE 8. COMPARISON OF NUMERICAL PREDICTIONS (FULL SYMBOLS) VS EXPERIMENTAL MEASUREMENTS (EMPTY SYMBOLS) OF THE PERFORMANCE OF THREE TURBINES PLACED WITH A LATERAL OFFSET OF 0.25D, AND A DOWNSTREAM SEPARATION OF 5D. FRONT TURBINE: BLUE SYMBOLS, MIDDLE TURBINE: BLACK SYMBOLS, DOWNSTREAM TURBINE: RED SYMBOLS.

The efficiency decreases with blockage ratio, quickly between 20% and 10%, and more slowly from 10% to 5%. The location of the peak efficiency also decreases in TSR value, becoming consistent with the theoretical predictions ($TSR_{opt} = 7 - 7.5$) for the upstream turbine. Interestingly, the value of the optimum TSR for the other two turbines in the array do not recover back to the theoretical prediction. The increase in efficiency with blockage ratio is also much more marked in the downstream turbines, specially in the downstream-most turbine, hinting at the cumulative effect that blockage ratio has on the subsequent rows of the array. As the front turbine creates a wake with a momentum deficit and accelerates the flow outside of it, the confinement is stronger for the following turbine as the effective cross section of the flume is reduced by the cross section of the low momentum flow in the wake. As more turbines add to the low momentum wake, further turbines downstream feel an increasingly confined environment where more flow is forced to pass through the rotor disk, leading to higher power extraction.

SUMMARY AND FUTURE WORK

The flow field and energy extraction in a small array of MHK turbines has been investigated through experiments and simulations at a laboratory scale. A turbine that is similar performance-wise (identical Cp vs TSR) to the DOE RM1 has been designed, built, instrumented and tested for flume experiments (scale 45:1). Numerical simulations based on the Blade Element Method have been performed and compared to the ex-

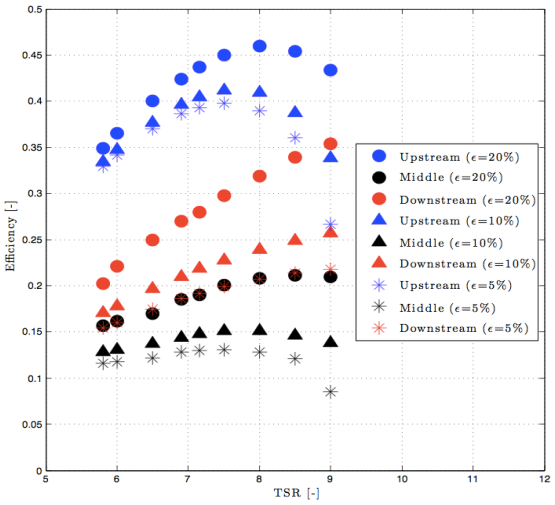

FIGURE 9. PERFORMANCE OF THREE TURBINES PLACED WITH A LATERAL OFFSET OF 0.25D, AND AT 5 DIAMETERS DOWNSTREAM SEPARATION, AS A FUNCTION OF THE BLOCKAGE RATIO IN THE COMPUTATIONAL DOMAIN.

perimental measurements. The performance is well represented in the simulations, particularly for the front turbine and at the optimum TSR. Flow separation along the blade span, apparent at low TSR values, makes the simulation results deviate from the experiments. Enhanced recovery of the wake in the experiments compared to the simulations is also apparent from the PIV velocity profiles across the wake and in the efficiency measured versus simulated. A high fidelity Large Eddy Simulation (LES) based on the open source SOWFA code developed at NREL is being implemented to improve the simulation's ability to capture the dynamics of the wake development and recovery in the flume (https://github.com/nnmrec/fastFlume).

ACKNOWLEDGMENT

This work was supported by DOE through a grant funding the National Northwest Marine Renewable Center (NNMREC) at OSU-UW.

REFERENCES

[1] Batten, W., Chaplin, J., Bahaj, A., and A., M., 2007. "Experimentally validated numerical method for hydrodynamic design of horizontal axis tidal turbines.". *Ocean Engineering,* ***34***, p. 1013.

[2] Batten, W., Chaplin, J., Bahaj, A., and A., M., 2008. "The prediction of the hydrodynamic performance of marine current turbines.". *Renewable energy,* ***33***, p. 1085.

[3] Lawson, M., Li, Y., and Sale, D., 2011. "Development and verification of a computational fluid dynamics model of a horizontal-axis tidal current turbine". In Proceedings of the 30th International Conference on Ocean, Offshore, and Arctic Engineering.

[4] Seokkoo Kang, S., Borazjani, I., Colby, J. A., and Sotiropoulos, F., 2012. "Numerical simulation of 3d flow past a real-life marine hydrokinetic turbine". *Advances in Water Resources*.

[5] Mycek, P., Gaurier., B., Pinon, G., and Rivoalen, E., 2011. "Numerical and experimental study of the interaction between two marine current turbines". In Proceedings of the 9th European Wave and Tidal Energy Conference.

[6] Bahaj, A., Molland, A., Chaplin, J., and Batten, W., 2007. "Power and thrust measurements of marine current turbines under various hydrodynamic flow conditions in a cavitation tunnel and a towing tank". *Renewable Energy,* ***32***(3), pp. 407 – 426.

[7] O'Doherty, T., Mason-Jones, A., ODoherty, D., Byrne, C., Owen, I., and Wang, Y., 2009. "Experimental and computational analysis of a model horizontal axis tidal turbine". In 8th European Wave and Tidal Energy Conference (EWTEC), Uppsala, Sweden.

[8] Maganga, F., Germain, G., King, J., Pinon, G., and Rivoalen, E., 2010. "Experimental characterisation of flow effects on marine current turbine behaviour and on its wake properties". *Renewable Power Generation, IET,* ***4***(6), pp. 498–509.

[9] Stelzenmuller, N., 2013. "Marine hydrokinetic turbine array performance and wake characteristics". Master's thesis, University of Washington.

[10] Lissaman, P., 1983. "Low-reynolds-number airfoils". *Annual Review of Fluid Mechanics,* ***15***, pp. 223–239.

[11] Sale, D., 2010. Harp_opt user's guide. Tech. rep., National Renewable Energy Laboratory, http://wind.nrel.gov/designcodes/simulators/HARP_Opt/.

[12] Javaherchi, T., 2010. "Numerical modeling of tidal turbines: Methodology development and potential physical environmental effects". Master's thesis, University of Washington.

[13] Javaherchi, T., and Aliseda, A., 2014. "Hierarchical methodology for the numerical simulation of the flow field around and in the wake of horizontal axis wind turbines: Rotating reference frame, blade element method and actuator disk model.". *Wind Engineering,* ***38***(2), pp. 61–82.